Effect of Exosomes From Bone Marrow–Derived Mesenchymal Stromal Cells and Adipose-Derived Stromal Cells on Bone-Tendon Healing in a Murine Rotator Cuff Injury Model

Xiaoqian Tan,*†‡ MD, Han Xiao,*†‡ PhD, An Yan,*†‡ MD, Miao Li,*†‡ PhD, and Linfeng Wang,§‖ MD
Investigation performed at Hunan Children's Hospital, Changsha, Hunan, China

Background: Bone-tendon injury is characterized by poor self-healing. It is established that exosomes are favorable for tissue repair and regeneration. However, their effect on bone-tendon healing has not yet been determined.

Purpose: To compare the effectiveness of exosomes derived from adipose-derived mesenchymal stromal cells (ADSC-Exos) and bone marrow–derived mesenchymal stromal cells (BMSC-Exos) on bone-tendon interface healing in murine rotator cuff injury model and explore the underlying mechanisms thereof.

Study Design: Controlled laboratory study.

Methods: A total of 63 male C57BL6 mice with rotator cuff injuries underwent surgery and were randomly assigned to a control group treated without exosomes (n = 21), an ADSC-Exos group (n = 21), or a BMSC-Exos group (n = 21). The mice were sacrificed 4 or 8 weeks after surgery, and tissues were collected for histologic examination and radiographic and biomechanical testing. For exosome tracing in vivo, mice were sacrificed 7 days after surgery. A series of functional assays (radiographic evaluation, proliferation assay, Alizarin Red staining, alkaline phosphatase staining and activity, Alcian blue staining, quantitative polymerase chain reaction analyses, and glycosaminoglycans quantification) were conducted to evaluate the effect of exosomes on the cellular behaviors of the BMSCs in vitro. A statistical analysis of multiple-group comparisons was performed by 1-way analysis of variance, followed by the Bonferroni post hoc test to assess the differences between the 2 groups.

Results: The ADSCs and BMSCs were positive for surface markers CD29 and CD90 and negative for surface markers CD34 and CD45 and could differentiate into osteoblasts, chondrocytes, and adipocytes. Exosomes showed a cup- or sphere-shaped morphology and were positive for CD63 and TGS101. Local injection of ADSC-Exos and BMSC-Exos could recruit BMSCs and promote osteogenesis, chondrogenesis, and bone-tendon healing. In vitro, ADSC-Exos and BMSC-Exos could significantly promote the proliferation, migration, osteogenic differentiation, and chondrogenic differentiation ability of BMSCs. In vivo, ADSC-Exos and BMSC-Exos significantly accelerated bone-tendon injury healing, with no significant statistical difference between them.

Conclusion: ADSC-Exos and BMSC-Exos exhibited similar therapeutic effects on bone-tendon healing in our murine animal model.

Clinical Relevance: ADSC-Exos and BMSC-Exos may be used to develop a new cell-free therapy method for promoting rotator cuff injury repair.

Keywords: adipose-derived mesenchymal stromal cell; bone marrow–derived mesenchymal stromal cell; bone-tendon healing; exosomes; rotator cuff

Rotator cuff injury is considered a bone-tendon interface (BTI) injury and is common in modern sports activities. It often causes severe clinical symptoms, such as pain and dysfunction of the shoulder.[23] Surgical repair has

The Orthopaedic Journal of Sports Medicine, 12(1), 23259671231210304
DOI: 10.1177/23259671231210304

been a well-established and commonly accepted treatment for severe rotator cuff tear, while reports have shown that the structural failure of rotator cuff surgical repair varies[9,24] from 13% to 94%. Despite a dramatic increase in the number of studies per year, there is little evidence that the results of rotator cuff repair are improving.[33]

The BTI consists of 4 continuous tissue layers: (1) bone, (2) calcified fibrocartilage, (3) uncalcified fibrocartilage, and (4) tendon.[17,19] The microstructure of the BTI can be very effective in transferring muscle force to bone.[3] However, surgical repair of the rotator cuff has not been shown to recreate the microstructure of the BTI.[15] The fibrocartilaginous transition zone is often replaced by fibrovascular scar tissue, leading to BTI repair failure.[32]

Mesenchymal stromal cells (MSCs) have emerged as a powerful tool to promote tissue healing of their multipotential differentiation, self-renewal abilities, and immunomodulation.[29,30] Previously, bone marrow–derived mesenchymal stromal cells (BMSCs) and adipose-derived mesenchymal stromal cells (ADSCs) have shown promising experimental results in tissue wound healing.[8,21] However, there are still some problems regarding the safe application of cell therapy, such as tumor formation, thrombosis, and unwanted immune response.[11,14] With the in-depth research of MSCs, the efficacy of many MSC-based treatments can also be attributed to their paracrine action.[16] Exosomes—40 to 150 nm small membrane particles released from multiple cells—have been of increased interest in regenerative medicine.[7] By transporting microribonucleic acid, messenger RNA, deoxyribonucleic acid (DNA), proteins, and soluble molecules to target cells, exosomes regulate the eventual fate of recipient cells.[10] Several studies have confirmed that MSC-derived exosomes (MSC-Exos) can exert a similar effect to MSCs and avoid many of the risks associated with MSCs transplantation.[2] Thus, MSC-Exos may be represented as a new potential treatment for bone-tendon healing.

Considering that BMSCs have stronger osteogenic and chondrogenic differentiation ability, BMSC-Exos can show a better ability to increase the healing of rotator cuff injury, and BMSC-Exos can be used to develop a new cell-free therapy method for promoting rotator cuff injury repair. This study aimed to compare the therapeutic effectiveness between exosomes from ADSCs (ADSC-Exos) and BMSCs (BMSC-Exos) in a murine rotator cuff injury model and explore the underlying mechanism. We hypothesized that both exosomes from the 2 types of MSCs would be able to promote BTI healing.

METHODS

Study Groups

The study protocol was approved by the animal care and use committee of our institute. A total of 63 male C57BL6 mice, 6 to 8 weeks old, were used in this study. The mice were randomly assigned to 1 of 3 groups using a computer-based random order generator to establish rotator cuff injury models: a control group treated without exosomes (n = 21), an ADSC-Exos group (n = 21), or a BMSC-Exos group (n = 21). The mice were sacrificed 4 or 8 weeks after surgery, and tissues were collected for histologic examination (3 mice per group per time point) and radiographic and biomechanical testing (6 mice per group per time point). For exosomes tracing in vivo, mice were sacrificed 7 days after surgery (3 mice per group). Any animals that died before the expected sacrifice time point were excluded.

Cell Isolation and Identification

The ADSCs and BMSCs of the mice were isolated and cultured as previously described.[6,26] The isolated MSC cells of the mice were seeded into a 25-cm^2 culture flask and incubated at 37°C with 5% CO_2. Cells were passaged when they reached 80% to 90% confluence. The expression of the surface makers—including CD29 and CD90, which were always high in the MSC, and CD34 and CD45, which were always negative in the MSC on passage 3 or 4 cells—was tested by flow cytometry. All antibodies were purchased from BioLegend. The multilineage differentiation capacity of MSC—including adipogenesis, osteogenesis, and chondrogenesis—was detected using adipogenic, osteogenic, and chondrogenic media, respectively (Cyagen Biosciences).

Exosome Isolation, Identification, and Treatment

ADSCs or BMSCs were cultured in the exosome-free medium for 48 hours to isolate exosome particles. The

‖Address correspondence to Linfeng Wang, MD, Xiangya Hospital, Central South University, No. 87, Xiangya Road, Kaifu District, Changsha, 410008, China (email: 525311592@qq.com).

*Department of Pediatric Orthopedics, Hunan Children's Hospital, Changsha, Hunan, China.

†The School of Pediatrics, University of South China, Changsha, Hunan, China.

‡Hunan Provincial Key Laboratory of Pediatric Orthopedics, Hunan Children's Hospital, Hunan, China.

§Department of Sports Medicine, Xiangya Hospital, Central South University, Changsha, China.

X.T. and H.X. contributed equally to this article.

Final revision submitted December 16, 2022; accepted June 6, 2023.

One or more of the authors has declared the following potential conflict of interest or source of funding: Research support was received from the National Key Clinical Specialty Construction Project at Pediatric Surgery of Hunan Children's Hospital (XWYF [2022] No. 2), the Hunan Province Science and Technology Innovation Plan Project (2021SK50516), and the 440 Young Talents of 1233 program of Hunan Children Hospital. AOSSM checks author disclosures against the Open Payments Database (OPD). AOSSM has not conducted an independent investigation on the OPD and disclaims any liability or responsibility relating thereto.

Ethical approval for this study was obtained from the Animal Care and Use Committee of Hunan Children's Hospital (ref No: HCHDWLL-2022-16).

culture medium was collected. After centrifugation to remove the dead cells or cell debris, the supernatant was filtered using a 0.22-μm filter (Biosharp) and subjected to ultracentrifugation at 100,000*g* for 4 to 6 hours at 4°C. Exosomes congregated at the bottom of the tube were then washed and resuspended in phosphate-buffered saline (PBS). For exosomes identification, the CD63 and TSG101 expressions were detected by Western blotting, size distribution and concentration by NanoSight analysis (Particle Metrix), and morphology by transmission electron microscopy imaging (Hitachi H7500 TEM).

For the in vitro assay, cells were treated with exosomes based on 2 μg of exosomes per 1×10^5 of recipient cells. During the in vivo experiments, 20 μg of exosomes were injected into recipient mice via local injection (between the tendon and tuberosity with a 30-gauge insulin syringe) once a week for 4 weeks. An equal volume of exosomes diluent (PBS) was used as a control.

Rotator Cuff Injury Repair Model and Treatment

The surgery was conducted using a previously reported protocol.[13] After anesthetization with pentobarbital (0.6 mL/20 g; Sigma-Aldrich), a longitudinal skin incision was made to expose the deltoid muscle of the left shoulder, and a transverse cut was made on it. The acromion was retracted to expose the supraspinatus tendon. After the supraspinatus tendon was grasped with No. 6-0 Prolene (Ethicon), it was sharply transected at the insertion site on the greater tuberosity, and the fibrocartilage layer was removed with a scalpel blade. A bone tunnel was made transversely to the distal greater tuberosity. Then, the suture was passed through the drilled hole and tied to the supraspinatus tendon to its anatomic position. The mice were given intramuscular buprenorphine for analgesia 24 hours after the operation (0.1 mg/kg body weight) and allowed free cage activities. When the mice were sacrificed at postoperative weeks 4 or 8, the supraspinatus-humeral head composites were harvested.

Immunofluorescence

The MSC-Exos was labeled with a lipophilic fluorescent dye (DiR; Invitrogen) to detect their biodistribution in vivo using an in vivo fluorescence imager (IVIS Spectrum). To evaluate the effect of exosomes on BMSCs in vivo, BMSCs labeled with enhanced green fluorescent protein using lentivirus (Cyagen Biosciences) were injected into the humeral of mice at a density of 1×10^6. After 2 weeks of treatment, the mice were sacrificed for immunofluorescence staining as previously described.[27] Primary antibodies anti-GFP (1:400) and secondary antibodies (1:500) were purchased from Abcam. Finally, the slices were sealed with DAPI (4′,6-diamidino-2-phenylindole) and observed with a fluorescence microscope (Zeiss).

Radiographic Evaluation

Supraspinatus-humeral-head composite specimens were fixed in 4% formaldehyde. The microarchitecture of the trabecular bone surrounding the tendon attachment site was evaluated by Xradia 410 versa (Zeiss). The beam energy, power, exposure time, and sample-to-detector distance were separately set at 80.0 keV, 10 W, 1 second, and 4.0 cm, respectively. A total of 2401 radiographic projections were imaged by a charge-coupled device detector with a pixel size of 3.2 μm. Morphological parameters of the trabecular bone surrounding the tendon attachment site, such as the ratio of bone volume to total volume (BV/TV) and trabecular thickness (Tb. Th), were calculated by computed tomography analyzer software Version 1.11.

Histological Analysis

Fixed samples were decalcified in ethylenediaminetetraacetic acid, dehydrated in ethanol solutions, embedded in paraffin, and then cut into 5-μm slices. The sections were stained with hematoxylin and eosin (H&E) for general histology and with toluidine blue/fast green to assess fibrocartilage regeneration. Two experienced observers (L.W. and A.Y.)—involved in BTI studies for at least 5 years and blinded to treatment groups—measured the histological tendon maturing score.

Biomechanical Testing

Specimens from both groups harvested at each time point were used for biomechanical testing by a mechanical testing machine (MTS insight; MTS Systems). The specimen was loaded to failure at a 1 mm/min rate. The failure load and stiffness data were recorded.

Exosomes Uptake by BMSCs

Exosomes were labeled with a red fluorescent dye (PKH26; Sigma) according to the manufacturer's instruction; then, they were incubated with BMSCs at 37°C, 5% CO_2 for 3 hours. Next, the cells were washed with PBS and fixed in 4% paraformaldehyde for 15 minutes. After being washed 3 times with PBS, the BMSCs were stained with DAPI (0.5 μg/mL; Invitrogen) and detected using fluorescence microscopy (Zeiss).

Proliferation Assay

The proliferation rate of cells was detected with Cell Counting Kit–8 (CCK-8, MULTI SCIENCES). Cells (1000 cells/well) were seeded into a 96-well plate. On days 1, 3, 5, and 7, CCK-8 reagent (10 μL) was added to the media. After incubation for another 3 hours, the optical density of each well was measured at 450 nm using a microplate reader (Bio-Rad 680).

Migration Assay

For the Transwell assay, 1×10^4 cells were resuspended in a 100-μL minimum essential medium with 5% fetal bovine serum and were loaded into the upper chamber of a 24-well

TABLE 1
Oligonucleotides Used in the qRT-PCR[a]

Gene	Forward	Reverse
ALP	AGGGTGGACTACCTCTTAGGTC	AGGGTGGACTACCTCTTAGGTC
Osteocalcin	CCATCTTTCTGCTCACTCTGC	GGACTGAGGCTCCAAGGTAG
RUNX2	GACTGTGGTTACCGTCATGGC	ACTTGGTTTTTCATAACAGCGGA
SOX9	GTGGATGTCGAAGCAGCAG	CTCAGCTGCTCCGTCTTGAT
Col2A1	GGTGTCAAGGGTCACAGAGG	CACTCTCACCCTTCACACCC
Aggrecan	ACCTGTGTGAGATCGACCAG	GGAGTGACAATGCTGCTCAG
β-Actin	GGAGATCACAGCTCTGGCT	GTCGATTGTCGTCCTGAGG

[a]*ALP*, alkaline phosphatase; *β-actin*, beta-actin; *Col2A1*, collagen type 2 alpha 1 chain; qRT-PCR, quantitative real-time polymerase chain reaction; *RUNX2*, runt-related transcription factor 2; *SOX9*, SRY-box transcription factor 9.

transwell plate (Corning) with 8-μm pore-sized filters. A complete medium (containing 10% fetal bovine serum) supplemented with ADSC-Exos, BMSC-Exos, or isopycnic PBS was added to the lower chamber. After 12 hours of incubation, cells that migrated to the lower surface of the filter were rinsed, fixed, and stained with 1% crystal violet. An optical microscope was used to photograph and count the migrated cells.

For scratch wound assay, cells (2×10^5 cells/well) were seeded into a 12-well plate and cultured until a cell monolayer formed. A straight scratch was produced using a pipette tip. After being washed with PBS to remove floating cells, adherent cells were cultured, and wound closure was imaged at the 0, 12, and 24 hours of incubation. The rate of wound closure was calculated as follows: migration rate (%) = $(A_0 - A_n)/A_0 \times 100$, where A_0 represents the initial wound area and A_n represents the remaining area of a wound at the appointed time.

Alizarin Red Staining

After 3 weeks of osteogenic induction, cell samples were fixed in 4% paraformaldehyde for 30 minutes and stained with Alizarin Red for 5 minutes at room temperature. After washing twice with PBS, staining cells were imaged under a stereomicroscope. To quantify Alizarin Red staining, the mineralized nodules were dissolved in 10% cetylpyridinium for 20 minutes, and the absorbance of the solution was detected at 560 nm.

ALP Staining and Activity

After 7 days of osteogenic induction, the cell culture supernatants were collected for the alkaline phosphatase (ALP) activity assay using an ALP activity assay kit (Jiancheng Bioengineering) according to the manufacturer's instructions. ALP staining was conducted according to the BCIP/NBT Alkaline Phosphatase Color Development Kit protocol (Beyotime Institute of Biotechnology).

Alcian Blue Staining

Macromass was fixed in 4% paraformaldehyde for 12 hours, dehydrated with gradient ethanol, washed in butanol, and embedded in paraffin. Sections with a thickness of 5 μm were cut, which were then stained with an alcian blue solution. Imaging was obtained with a light microscope.

Glycosaminoglycans Quantification

According to the manufacturer's instructions, glycosaminoglycans (GAG) content among chondrogenic-differentiating cells was determined using an Acidic Mucopolysaccharide Kit (K-Assay). The cell pellet was digested thoroughly using an enzyme solution at 60°C for an hour. After cooling, the 100 μL of digested tissue was thoroughly mixed with 1.3 mL of the staining stock solution. The absorption of the solution at 650 nm was measured within 20 minutes of mixing. Each sample's GAG concentration was calculated using a standard curve generated by the chondroitin sulfate calibrator. The DNA content in the lysate was measured using a PicoGreen dsDNA quantitation assay (YEASEN). The GAG content was then normalized to the DNA content.

qRCR Analyses

Total RNA was isolated using Trizol reagent (Invitrogen) and then synthesized cDNA with GoScript Reverse Transcription System (Promega). The quantitative real-time polymerase chain reaction (qRT-PCR) was conducted on the ABI PRISM 7900HT System (Applied Biosystems) with GoTaq qPCR Master Mix (Promega). The relative gene expression was calculated using the $2^{-\Delta\Delta CT}$ method, and β-actin was used as an internal control for normalization. The details of primer sequences used for qRT-PCR are shown in Table 1.

Statistical Analysis

All data were reported as means and standard deviations. GraphPad Prism software (GraphPad) was used for the statistical procedure. Statistical analysis of multiple-group comparisons was performed by 1-way analysis of variance, followed by the Bonferroni post hoc test to assess the

significance of differences between the 2 groups. Statistically significant differences were considered when $P < .05$.

RESULTS

Identification of ADSCs, BMSCs, and Exosomes

ADSCs and BMSCs showed a spindle-like morphology (Figure 1A). After being cultured in a differentiation medium, they exhibited strong capacities to differentiate into osteoblasts, chondrocytes, and adipocytes, as confirmed by Alizarin Red staining, Oil Red O staining, and Alcian blue staining (Figure 1A). Flow cytometry showed that 2 types of MSCs were highly positive for CD29 and CD90 but negative for CD34 and CD45 (Figure 1B).

Transmission electron microscopy and Western blot analysis were used to identify the purified nanoparticles derived from ADSCs and BMSCs (Figure 1C). We found that ADSC-Exos and BMSC-Exos exhibited a cup- or sphere-shaped morphology, with a mean diameter of 130 ± 2.5 mm and 127.5 ± 1.9 mm, respectively (Figure 1D). Western blot analysis showed that CD63 and TSG101 were positive in ADSC-Exos and BMSC-Exos (Figure 1E).

MSC-Derived Exosomes and Healing of Mouse Rotator Cuff Injury

In vivo, fluorescence imaging analysis showed that MSC-Exos was able to exist in the injury site for about 1 week (Figure 2A). Immunofluorescence analysis showed that GFP^+ BMSCs were recruited to the injury site, which was involved in the healing of the BTI (Figure 2B).

At 4 weeks after surgery, H&E (Figure 3A) and Toluidine Blue and Fast-Green (Figure 3B) staining showed highly cellular fibrovascular granulation tissue at the supraspinatus BTI in all groups. The histological scores were 18.7 ± 0.6 in the ADSC-Exos group, 18.3 ± 0.6 in the BMSC-Exos group, and 15 ± 1 in the control group. There was a significant difference between the exosomes-treated group and the control group ($P < .05$ for all) but no difference between BMSC-Exos and ADSC-Exos groups ($P > .05$). In the BSMC-Exos group and ADSC-Exos group, we found that the fibrovascular scar was relatively organized. The well-organized soft tissue at the BTI in all groups with tide markers occurred at 8 weeks. There were also significant cells decreasing from 4 to 8 weeks. The histological scores were 24 ± 1 in the ADSC-Exos group, 23.3 ± 0.6 in the BMSC-Exos group, and 21.7 ± 0.6 in the control group. There was a significant difference between the exosomes-treated group and the control group ($P < .05$ for all) but no significant difference between BMSC-Exos and ADSC-Exos groups ($P > .05$).

The Xradia radiographic evaluation showed that ADSC-Exos and BMSC-Exos groups had a better quality of bone around the injury surface than the control group at postoperative 4 weeks and 8 weeks (Figure 4, A and B, and Table 1). The BV/TV and Tb.Th in the MSCs-Exos groups at both time points were significantly higher than in the control group ($P < .05$ for all); however, no significant difference was found between exosome groups ($P > .05$).

During the mechanical testing, all specimens were torn at the BTI. At postoperative 4 weeks, the ADSC-Exos and BMSC-Exos groups exhibited a higher failure load and stiffness when compared with the control group ($P < .05$ for both). Still, no significant difference was found between the 2 exosomes-treated groups ($P > .05$) (Figure 4C and Table 2). The mechanical strength (failure load and stiffness) of the BTI improved from postoperative weeks 4 to 8 weeks in all groups. However, the values of failure load and stiffness in the control group were significantly lower at week 8 than in the 2 exosome-treated groups ($P < .05$ for both), with no significant difference between the 2 exosome-treated groups ($P > .05$) (Figure 4C and Table 2).

MSC-Derived Exosomes and BMSC Proliferation, Migration, and Differentiation Abilities

We then compared the impact of the 2 exosomes on BMSCs. After 3 hours of cocultivation, using fluorescence microscopy, we could see that PKH26 labeled exosomes were incorporated into BMSCs (Figure 5A). The CCK-8 assay showed that both kinds of exosomes could improve the proliferative ability of BMSCs (day 7: control [0.88 ± 0.01] vs ADSC-Exos [1.03 ± 0.01], $P < .05$; control [0.88 ± 0.01] vs BMSC-Exos [1.02 ± 0.02]; $P < .05$) (Figure 5B). However, no significant difference was observed between them ($P > .05$ for both). BMSCs in ADSC-Exos and BMSC-Exos groups exhibited stronger migration ability than the control group, as evidenced by the Transwell migration assay (control [54.7 ± 3.1] vs ADSC-Exos [180 ± 13.2]; $P < .05$; control [54.7 ± 3.1] vs BMSC-Exos [198.3 ± 24.8]; $P < .05$) (Figure 5C, 5D) and scratch wound assay (at 24 hours: control [61.2 ± 1.4] vs ADSC-Exos [86.6 ± 2.4]; $P < .05$; control [61.2 ± 1.4] vs BMSC-Exos [89.1 ± 2.9]; $P < .05$) (Figure 5, E and F). No significant difference was observed between the ADSC-Exos and BMSC-Exos groups ($P > .05$ for both).

To analyze the chondrogenic and osteogenic stimulative abilities of the MSC-Exos, we cultivated BMSCs in a chondrogenic or osteogenic induction medium supplemented with ADSC-Exos, BMSC-Exos, or an equal volume of PBS. We found that the exosomes-treated groups showed greater osteogenic (Figure 6, A-C) and chondrogenic (Figure 6, C-E) abilities when compared with the control group. No significant difference was found between the 2 exosome-treated groups ($P > .05$).

DISCUSSION

The main finding of this study is that BMSC-Exos and ADSC-Exos can effectively promote early healing quality of rotator cuff injury in our murine animal model. The BMSC-Exos and ADSC-Exos-treated groups appeared to have better quality new remodeling bone, well-organized collagen fibers, and thicker fibrocartilage in the regenerated BTI zone at postoperative 4 and 8 weeks. Meanwhile,

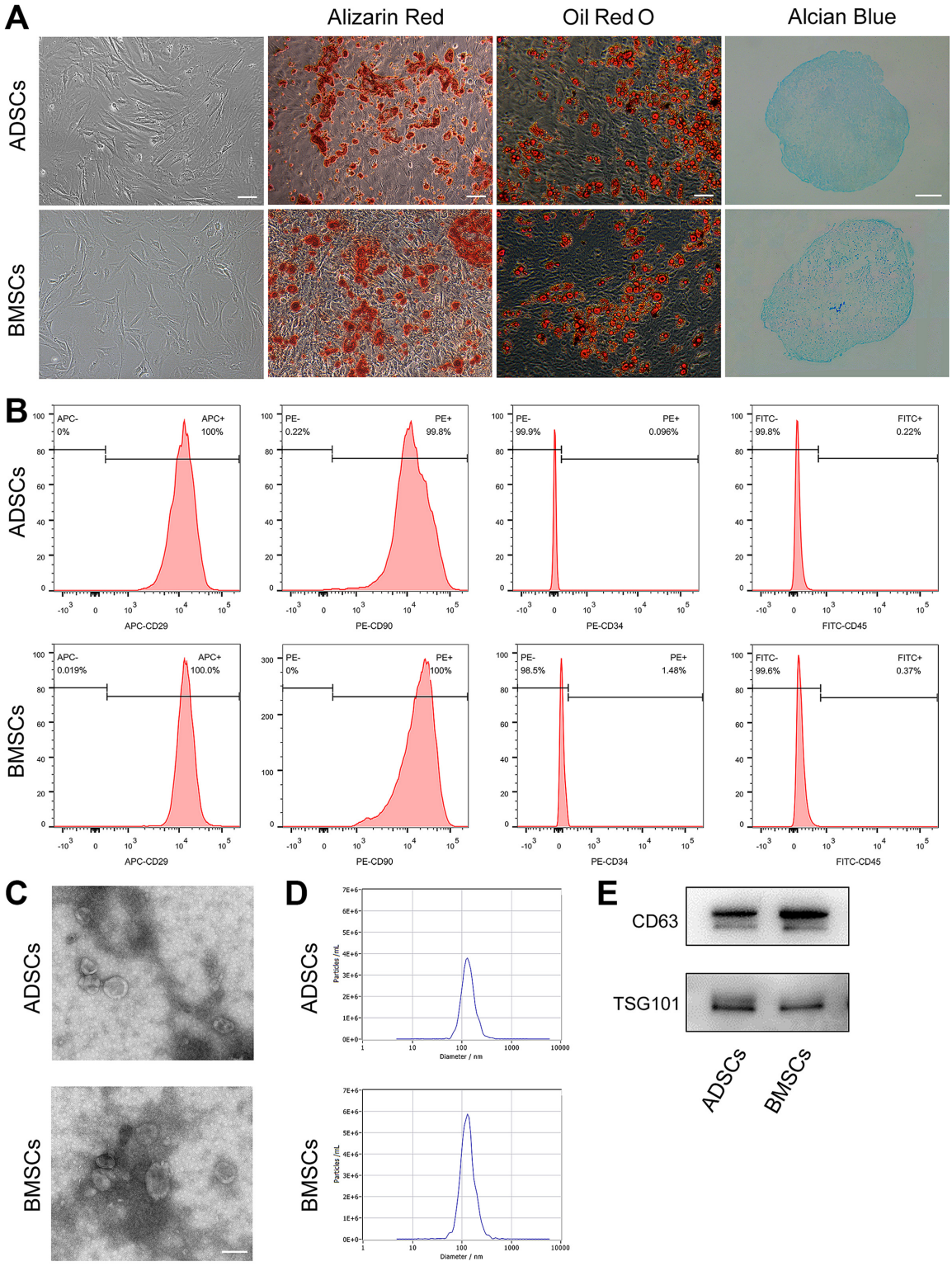

Figure 1. Identification of ADSCs and ADSC-Exos. (A) Identification of MSCs by optical morphology (scale bar: 100 μm), Alizarin Red staining (scale bar: 100 μm), Oil Red O staining (scale bar: 50 μm), and Alcian blue staining (scale bar: 200 μm). (B) Results of flow cytometry analysis. (C) Morphology of ADSC-Exos under a transmission electron microscope (scale bar: 200 nm). (D) Size distribution profile of AMSC-Exos. (E) Western blot analysis of exosome-specific CD63 and TSG101 proteins. ADSCs, adipose-derived mesenchymal stromal cells; MSCs, mesenchymal stromal cells.

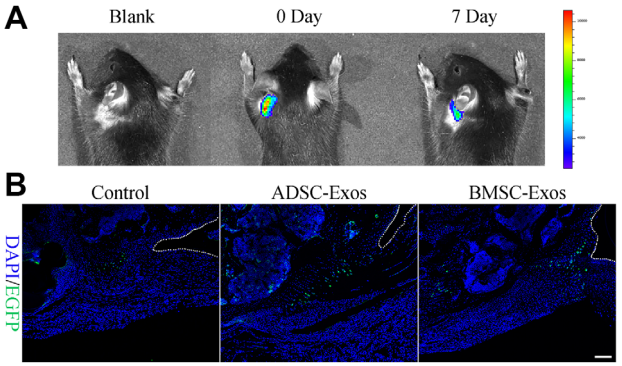

Figure 2. (A) DiR-labeled MSC-Exos existed in the injury site for about 1 week. (B) Cell tracking showed exogenous BMSCs could be recruited into the healing area (Scale bar = 100 μm). BMSCs, bone marrow–derived mesenchymal stromal cells; Exos, exosomes; MSCs, mesenchymal stromal cells.

both of the exosomes-treated groups indicate a high value of mechanical strength compared with the control group. In vitro, we found that BMSC-Exos and ADSC-Exos could effectively enhance the proliferation, migration, osteogenic differentiation, and chondrogenic differentiation of BMSCs.

There were other sources of MSCs, although we compared only the ADSC-Exos and BMSC-Exos in this study. Generally speaking, embryonic stem cells have a significant clinical advantage in differentiating into various cell types.[31] However, these stem cells are derived from embryos, which causes ethical issues.[28] At the same time, BMSCs and ADSCs are more accessible to isolated and cultured in vitro without ethical problems like embryonic stem cells. Further, the collection of these MSCs resulted in less trauma to the body; both are considered promising cells for clinical therapy.[12] Hence, we chose BMSCs and ADSCs as sources of exosomes.

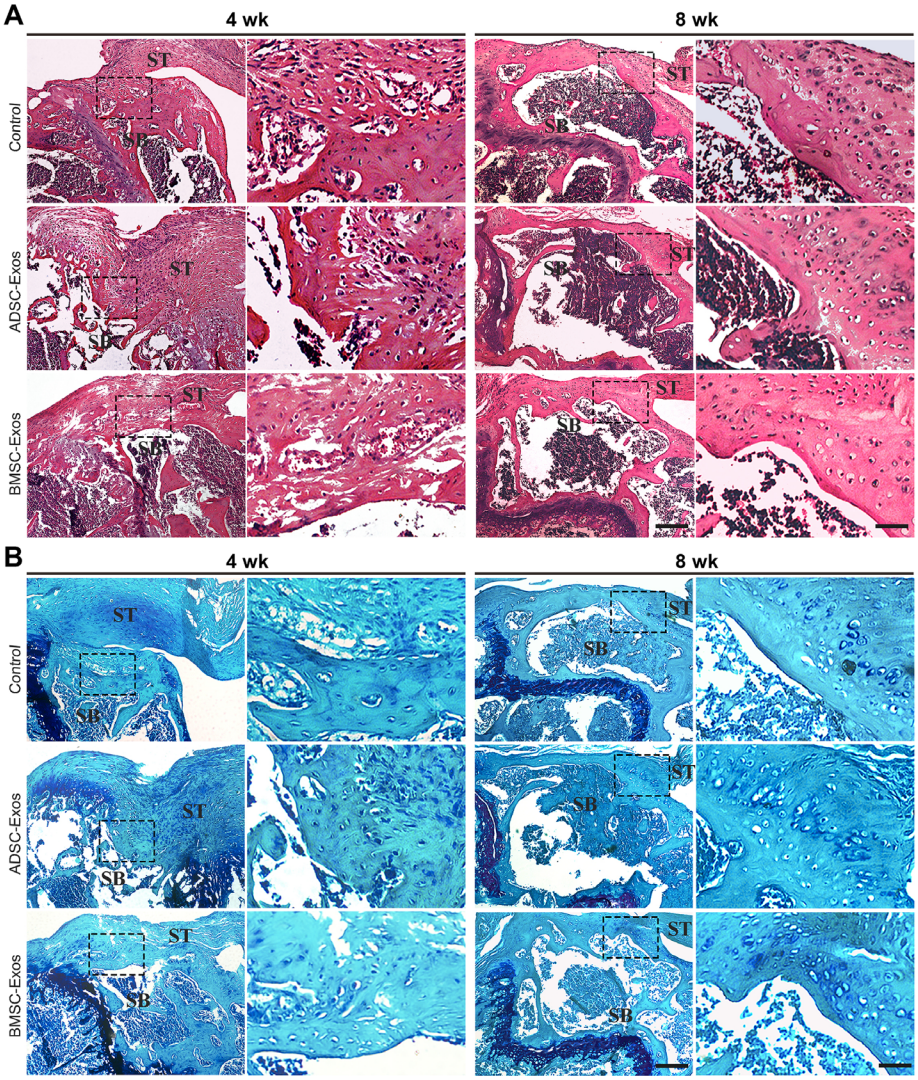

Figure 3. Histological evaluation of the bone-tendon interface. Representative (A) hematoxylin and eosin staining and (B) Toluidine Blue and Fast-Green staining of the bone-tendon interface at 4 and 8 weeks postoperatively in the control, ADSC-Exos, and BMSC-Exos groups (n = 3 per group). The ADSC-Exos and BMSC-Exos groups showed better healing results than the control group at postoperative 4 and 8 weeks (Scale bar: 50 μm). Dashed boxes represent the BTI; ADSCs, adipose-derived mesenchymal stromal cells; BMSCs, bone marrow–derived mesenchymal stromal cells; bone; Exos, exosomes; SB, subchondral; ST, supraspinatus tendon.

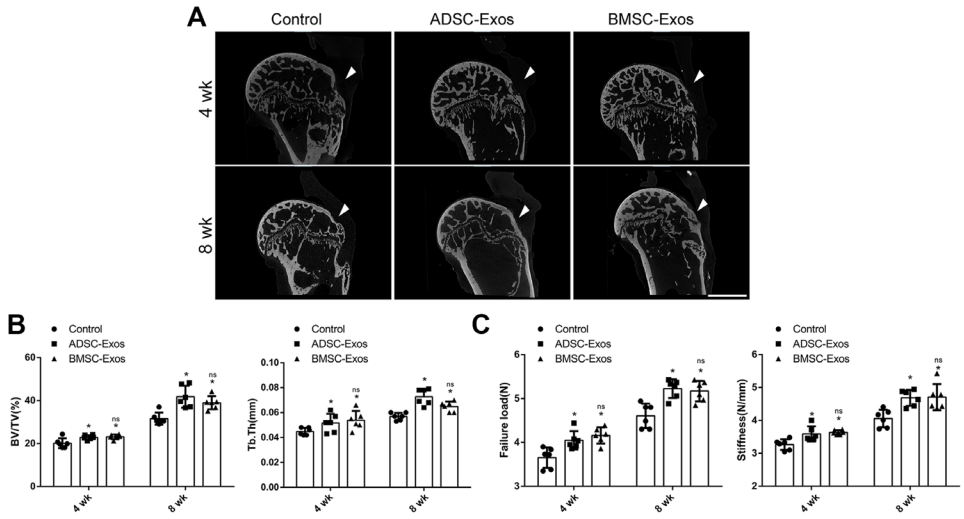

Figure 4. Radiographic evaluation and mechanical testing of BTI. (A) Representative Xradia tomography of the BTI at postoperative 4 and 8 weeks. The triangle indicated the BTI healing site (Scale bar: 1cm). (B) Comparison of BV/TV and Tb.Th around the injury site among 3 different groups (n = 6 per group). (C) Comparison of mechanical tests among the 3 groups (n = 6 per group). ADSCs, adipose-derived mesenchymal stromal cells; BMSCs, bone marrow–derived mesenchymal stromal cells; bone; BTI, bone-tendon interface; BV/TV, bone volume/tissue volume; Exos, exosomes; ns, not significant versus ADSC-Exos group; Tb.Th, trabecular thickness.
*Statistically significant difference versus controls ($P < 0.05$).

TABLE 2
Data on Radiographic Evaluation and Mechanical Testing of Bone-Tendon Interface[a]

		Exosomes Groups		
	Control	ADSC-Exos	BMSC-Exos	P^b
Radiographic evaluation				
4 wk postoperative				
BV/TV, %	20.1 ± 2.3	22.8 ± 1.1	23.1 ± 1.1	<.05
Tb.Th, mm	0.045 ± 0.003	0.053 ± 0.006	0.054 ± 0.007	<.05
8 wk postoperative				
BV/TV, %	31.6 ± 2.8	41.8 ± 5.1	39.0 ± 3.1	<.05
Tb.Th, mm	0.057 ± 0.003	0.071 ± 0.006	0.065 ± 0.004	<.05
Mechanical testing				
4 wk postoperative				
Failure load, N	3.6 ± 0.3	4.1 ± 0.2	4.1 ± 0.1	<.05
Stiffness, N/mm	3.3 ± 0.1	3.8 ± 0.2	3.6 ± 0.1	<.05
8 wk postoperative				
Failure load, N	4.6 ± 0.3	5.2 ± 0.3	5.2 ± 0.4	<.05
Stiffness, N/mm	4.1 ± 0.2	4.7 ± 0.2	4.7 ± 0.1	<.05

[a]ADSCs, adipose-derived mesenchymal stromal cells; BMSCs, bone marrow–derived mesenchymal stromal cells; bone; BV/TV, bone volume/tissue volume; Exos, exosomes; Tb.Th, trabecular thickness.
[b]*P* values for comparison of exosomes groups with the control group.

Transplanted MSCs can be involved in tissue repair by directly differentiating into corresponding tissue. At the same time, the MSCs also play an essential role in tissue homeostasis through direct cell-to-cell interaction, secreting particles or soluble molecules.[20] Sevivas et al[25] found that rotator cuff repair could benefit from BMSC secretome by culturing tenocytes in a human BMSC secretome, which contains many cytokines, growth factors, and vesicles released from BMSC. This finding suggested that MSC could promote rotator cuff repair by secreted substances via paracrine mechanisms or by modulating the local immune and bioactivity environment. It was well known that exosomes can transfer messages encoded in protein, lipids, messenger RNA, and microribonucleic acid enclosed within a lipid bilayer, which acts in an autocrine and paracrine manner.[1,5] The cell types regulate the contents of exosomes in response to the different microenvironments. In this study, we used BMSCs and ADSCs-derived

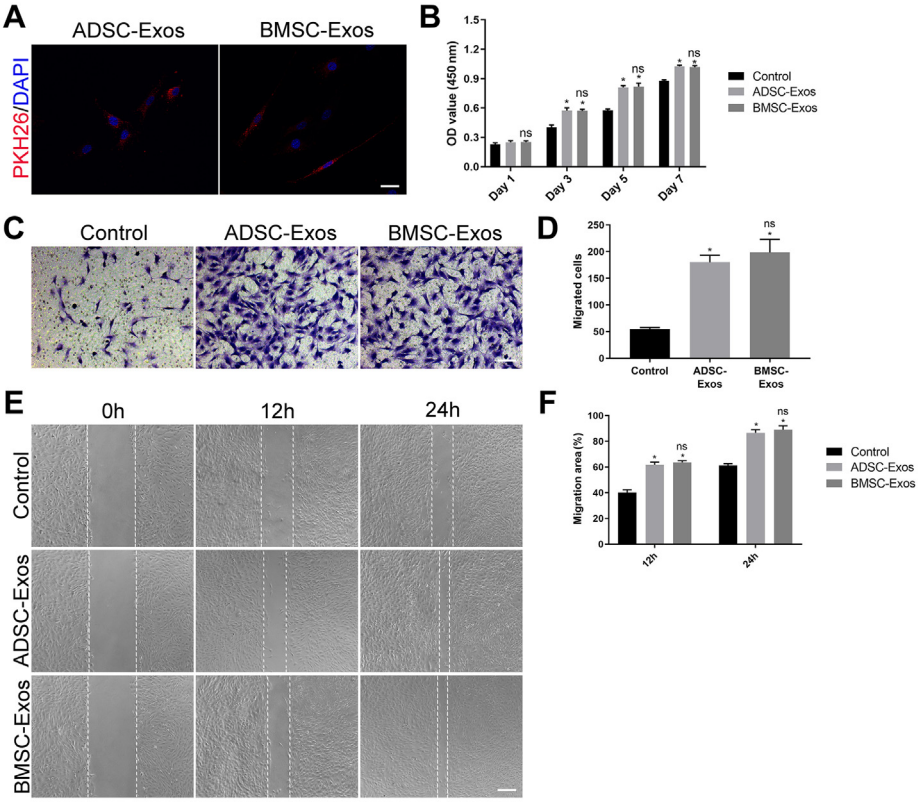

Figure 5. ADSC-Exos and BMSC-Exos promoted the proliferation and migration of BMSCs in vitro. (A) Internalization of PKH26-labeled ADSC-Exos or BMSC-Exos by BMSCs. The red-labeled exosomes were around the nucleus (scale bar: 50 μm). (B) The proliferation rate of BMSCs receiving different treatments was tested by CCK-8 (n = 3 per group). (C) Representative picture of Transwell assay in BMSCs treated with ADSC-Exos, BMSC-Exos, or PBS (scale bar: 100 μm). (D) Quantitative analysis of migrated cells in (C); n = 3 per group. (E) Representative picture of the scratch wound in BMSCs treated with ADSC-Exos, BMSC-Exos, or PBS (scale bar: 250 μm). (F) Quantitative analysis of migration rates in (E); n = 3 per group. ADSCs, adipose-derived mesenchymal stromal cells; BMSCs, bone marrow–derived mesenchymal stromal cells; Exos, exosomes; ns, not significant versus the ADSC-Exos group; OD, optical density.
*Statistically significant difference versus controls ($P < .05$).

exosomes treating rotator cuff injury. We found that these exosomes could augment new bone formation and fibrocartilage regeneration, eventually increasing the value of mechanical test value; however, no difference was found between these 2 exosomes. Combined with the in vitro experimental results that indicated these exosomes could promote the ability of BMSCs to proliferate, migrate, and differentiate into osteoblast and chondroblast, we considered that the direct activation of BMSCs may mediate the pro-BTI healing effect of MSC-Exos.

During rotator cuff repair, the perfect functional restoration was based on newly formed bone and the regenerated fibrocartilage layer, working together as the mediation and transfer for motility. According to a previous study, the area, length, and mineralization of newly formed bone at the rabbit BTI healing site positively correlate with its healing quality.[18] Meanwhile, the generation of fibrocartilage is crucial to the quality of BTI healing.[17] Our study found that the groups with high value of BV/TV and good quality of fibrocartilage in the BTI had better mechanical test results, which is consistent with previous literature.

BMSCs and ADSCs come from different tissues and play different roles in the physiological and pathological processes. In previous studies, BMSCs showed higher chondrogenic differentiation ability than ADSCs.[4,22] However, no difference was found in this study between these 2 groups. We hypothesize that once they are separated from the local environment and cultured in the same medium, their difference will shrink or disappear, and the exosomes will show no discrepancy between them in such conditions. Further studies will be needed to determine the mechanisms.

Limitations

This study has several limitations. First, the rotator cuff injury model we used in this study is a small animal model that may not fully mimic the process of human rotator cuff injury repair. Further studies with large animal models are needed to compare the effects between them. Second, our study focused on whether BMSC-Exos and ADSC-Exos could differentially promote rotator cuff healing and find the difference between them. Still, we did not

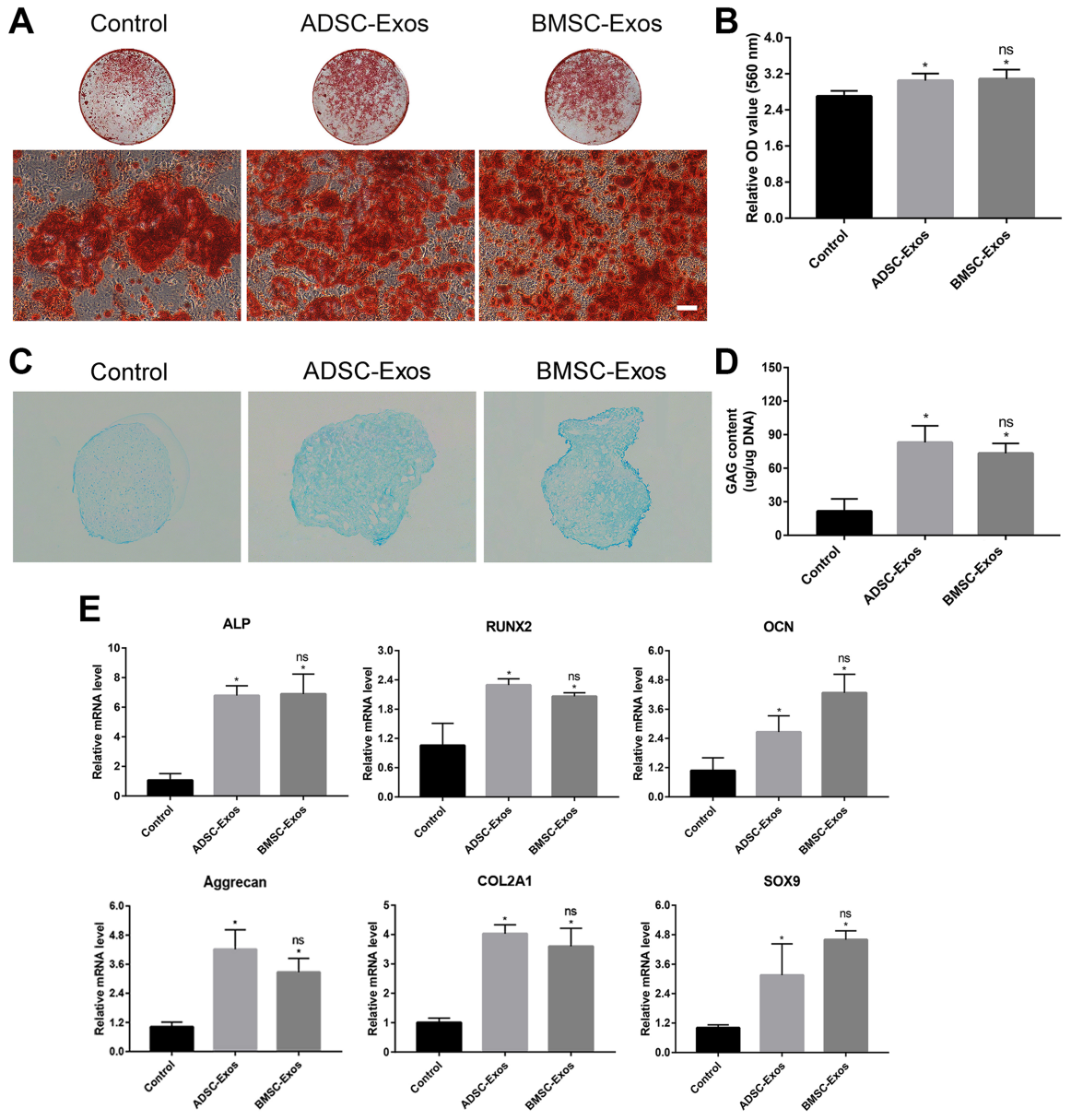

Figure 6. ADSC-Exos and BMSC-Exos promoted osteogenic and chondrogenic differentiation of BMSCs in vitro. (A) Representative images of Alizarin Red staining (scale bar: 100μm); (B) quantitative analysis of Alizarin Red staining in (A); n = 3 per group; (C) Representative images of Alcian blue staining; (D) quantitative analysis of GAG content, normalized to DNA content (n = 3 per group). (E) The osteogenesis and chondrogenesis-related gene expression by BMSCs induced in osteogenic or chondrogenesis medium supplemented with ADSC-Exos, BMSC-Exos, or PBS. ADSCs, adipose-derived mesenchymal stromal cells; ALP, alkaline phosphatase; BMSCs, bone marrow–derived mesenchymal stromal cells; *Col2A1*, collagen type 2 alpha 1 chain; DNA, deoxyribonucleic acid; Exos, exosomes; GAG, glycosaminoglycan; ns, not significant versus the ADSC-Exos group; PBS, phosphate-buffered saline; RUNX2, runt-related transcription factor 2; *SOX9*, SRY-Box Transcription Factor 9.
*Statistically significant difference versus controls ($P < .05$).

demonstrate the detailed factors in exosomes that played a vital role in rotator cuff healing. It still needs to be revealed in the future. Third, BMSCs were just 1 progenitor cell involved in rotator cuff repair. We did not trace its fate and other MSCs' role in the BTI. For example, we did not reveal the role of tendon stromal cells in the process.

CONCLUSION

The findings of this study revealed that the exosomes derived from BMSCs and ADSCs could enhance the functional properties of BMSCs and promote BTI healing in mouse rotator cuff injury. ADSC-Exos and BMSC-Exos

may be used to develop a new cell-free therapy method for promoting rotator cuff injury repair.

ACKNOWLEDGMENT

The authors thank the members of the Hunan Children's Hospital and Xiangya Hospital for their support during this study.

REFERENCES

1. Baglio SR, Rooijers K, Koppers-Lalic D, et al. Human bone marrow- and adipose-mesenchymal stem cells secrete exosomes enriched in distinctive miRNA and tRNA species. *Stem Cell Res Ther*. 2015;6:127.
2. Basu J, Ludlow JW. Exosomes for repair, regeneration and rejuvenation. *Expert Opin Biol Ther*. 2016;16:489-506.
3. Benjamin M, Toumi H, Ralphs JR, Bydder G, Best TM, Milz S. Where tendons and ligaments meet bone: attachment sites ('entheses') in relation to exercise and/or mechanical load. *J Anat*. 2006;208:471-490.
4. Cavallo C, Cuomo C, Fantini S, et al. Comparison of alternative mesenchymal stem cell sources for cell banking and musculoskeletal advanced therapies. *J Cell Biochem*. 2011;112:1418-1430.
5. Chaubey S, Thueson S, Ponnalagu D, et al. Early gestational mesenchymal stem cell secretome attenuates experimental bronchopulmonary dysplasia in part via exosome-associated factor TSG-6. *Stem Cell Res Ther*.2018;9:173.
6. Chen C, Liu F, Tang Y, et al. Book-shaped acellular fibrocartilage scaffold with cell-loading capability and chondrogenic inducibility for tissue-engineered fibrocartilage and bone-tendon healing. *ACS Appl Mater Interfaces*. 2019;11:2891-2907.
7. Chen CY, Rao SS, Ren L, et al. Exosomal DMBT1 from human urine-derived stem cells facilitates diabetic wound repair by promoting angiogenesis. *Theranostics*. 2018;8:1607-1623.
8. Degen RM, Carbone A, Carballo C, et al. The effect of purified human bone marrow-derived mesenchymal stem cells on rotator cuff tendon healing in an athymic rat. *Arthroscopy*. 2016;32:2435-2443.
9. Galatz LM, Ball CM, Teefey SA, Middleton WD, Yamaguchi K. The outcome and repair integrity of completely arthroscopically repaired large and massive rotator cuff tears. *J Bone Joint Surg Am*. 2004;86:219-224.
10. Hessvik NP, Llorente A. Current knowledge on exosome biogenesis and release. *Cell Mol Life Sci*. 2018;75:193-208.
11. Kizil C, Kyritsis N, Brand M. Effects of inflammation on stem cells: together they strive. *EMBO Rep*. 2015;16:416-426.
12. Koga H, Muneta T, Nagase T, et al. Comparison of mesenchymal tissues-derived stem cells for in vivo chondrogenesis: suitable conditions for cell therapy of cartilage defects in rabbit. *Cell Tissue Res*. 2008;333:207-215.
13. Lebaschi AH, Deng XH, Camp CL, et al. Biomechanical, histologic, and molecular evaluation of tendon healing in a new murine model of rotator cuff repair. *Arthroscopy*. 2018;34:1173-1183.
14. Lee HY, Hong IS. Double-edged sword of mesenchymal stem cells: cancer-promoting versus therapeutic potential. *Cancer Sci*. 2017; 108:1939-1946.
15. Leung KS, Chong WS, Chow DH, et al. A comparative study on the biomechanical and histological properties of bone-to-bone, bone-to-tendon, and tendon-to-tendon healing: an Achilles tendon-calcaneus model in goats. *Am J Sports Med*. 2015;43:1413-1421.
16. Liang X, Ding Y, Zhang Y, Tse HF, Lian Q. Paracrine mechanisms of mesenchymal stem cell-based therapy: current status and perspectives. *Cell Transplant*. 2014;23:1045-1059.
17. Lu H, Chen C, Qu J, et al. Initiation timing of low-intensity pulsed ultrasound stimulation for tendon-bone healing in a rabbit model. *Am J Sports Med*. 2016;44:2706-2715.
18. Lu H, Liu F, Chen H, et al. The effect of low-intensity pulsed ultrasound on bone-tendon junction healing: initiating after inflammation stage. *J Orthop Res*. 2016;34:1697-1706.
19. McGonagle D. Enthesitis: an autoinflammatory lesion linking nail and joint involvement in psoriatic disease. *J Eur Acad Dermatol Venereol*. 2009;23(suppl)1:9-13.
20. Morrison SJ, Spradling AC. Stem cells and niches: mechanisms that promote stem cell maintenance throughout life. *Cell*. 2008;132:598-611.
21. Oh JH, Chung SW, Kim SH, Chung JY, Kim JY. 2013 Neer Award: effect of the adipose-derived stem cell for the improvement of fatty degeneration and rotator cuff healing in rabbit model. *J Shoulder Elbow Surg*. 2014;23:445-455.
22. Park JS, Shim MS, Shim SH, et al. Chondrogenic potential of stem cells derived from amniotic fluid, adipose tissue, or bone marrow encapsulated in fibrin gels containing TGF-β3. *Biomaterials*. 2011;32:8139-8149.
23. Randelli PS, Menon A, Nocerino E, et al. Long-term results of arthroscopic rotator cuff repair: initial tear size matters: a prospective study on clinical and radiological results at a minimum follow-up of 10 years. *Am J Sports Med*. 2019:363546519865529.
24. Rhee YG, Cho NS, Yoo JH. Clinical outcome and repair integrity after rotator cuff repair in patients older than 70 years versus patients younger than 70 years. *Arthroscopy*. 2014;30:546-554.
25. Sevivas N, Teixeira FG, Portugal R, et al. Mesenchymal stem cell secretome improves tendon cell viability in vitro and tendon-bone healing in vivo when a tissue engineering strategy is used in a rat model of chronic massive rotator cuff tear. *Am J Sports Med*. 2018; 46:449-459.
26. Soleimani M, Nadri S. A protocol for isolation and culture of mesenchymal stem cells from mouse bone marrow. *Nat Protoc*. 2009;4:102-106.
27. Tang Y, Wu X, Lei W, et al. TGF-beta1-induced migration of bone mesenchymal stem cells couples bone resorption with formation. *Nat Med*. 2009;15:757-765.
28. Vogel G, Holden C. Stem cells. Ethics questions add to concerns about NIH lines. *Science*. 2008;321:756-757.
29. Wang Y, Chen X, Cao W, Shi Y. Plasticity of mesenchymal stem cells in immunomodulation: pathological and therapeutic implications. *Nat Immunol*. 2014;15:1009-1016.
30. Yang R, Liu F, Wang J, Chen X, Xie J, Xiong K. Epidermal stem cells in wound healing and their clinical applications. *Stem Cell Res Ther*. 2019;10:229.
31. Young RA. Control of the embryonic stem cell state. *Cell*. 2011; 144:940-954.
32. Zhang J, Yuan T, Zheng N, Zhou Y, Hogan MV, Wang JH. The combined use of kartogenin and platelet-rich plasma promotes fibrocartilage formation in the wounded rat Achilles tendon entheses. *Bone Joint Res*. 2017;6:231-244.
33. Zhang K, de Sa D, Kanakamedala A, Sheean AJ, Vyas D. Management of concomitant preoperative rotator cuff pathology and adhesive capsulitis: a systematic review of indications, treatment approaches, and outcomes. *Arthroscopy*. 2019;35:979-993.